INTERNATIONAL JOURNAL OF AUTOMOTIVE AND MECHANICAL ENGINEERING (IJAME)
ISSN: 2229-8649 e-ISSN: 2180-1606
VOL. 19, ISSUE 1, 9577 – 9592
DOI: https://doi.org/10.15282/ijame.19.1.2022.20.0739

ORIGINAL ARTICLE

Classification and Comparison of Crack and Dent Defects in a Metal Pipe Subjected to Variable Amplitude Loading

Zakaria Mighouar*, Hamza Khatib, Hammadi Chaiti, Laidi Zahiri and Khalifa Mansouri

SSDIA Laboratory, Hassan II University of Casablanca, ENSET of Mohammedia, Post Box No. 159, Mohammedia, Morocco

ABSTRACT – Pipelines are commonly used to transport energy over long distances. If this structure is subjected to an internal pressure of variable amplitude loading, such as water hammer waves, the structural damage caused by the presence of a defect can be exacerbated. Previous research by the authors resulted in the development of finite element models to evaluate crack and dent defects separately. Each model was used to compare and classify defects in their respective categories based on their nocivity in a metal pipe subjected to internal pressure. The primary objective of this paper is to compare the severity of various defect categories on the same scale. A numerical damage assessment model that considers the interaction effect, as well as the loading history, is used to achieve this goal. It takes the output of the two finite element models, as well as the pressure spectrum caused by the water hammer, as inputs. This model is used to analyze the effect of key parameters that influence the severity of the defects, as well as to compare and classify the various types of dent defects with the various types of crack defects found in pipes subjected to variable amplitude loading.

ARTICLE HISTORY
Received: 28th June 2021
Revised: 20th Dec 2021
Accepted: 18th Mar 2022

KEYWORDS
Damage accumulation;
Defect;
Harmfulness;
Pipeline;
Water hammer

INTRODUCTION

Pipelines are structures used primarily for the pressurized transport of flammable substances, which have higher safety requirements due to the risk of leakage or explosion [1]. New pipelines are needed to meet the growing demand for energy, such as gas and oil, among industrial users. Indeed, over the last 50 years, the latter has emerged as the most cost-effective and safest mode of long-distance transportation for large amounts of energy [2]. The length of pipelines in Europe was multiplied by four between 1970 and 2007. For the same time period, however, the failure rate was divided by six [2]. To improve the profitability of this mode of supply, manufacturers have increased both the operating pressure and the pipe diameter. Between 1910 and 2000, the largest pipeline's diameter increased fourfold, while transport pressure increased sixtyfold [3]. All of this was made possible by research that improved the mechanical properties of pipelines as well as tools that allow the severity of defects in these pipes to be assessed.

Undoubtedly, as with every metal structure, flaws in the pipeline may develop over time and cause it to rupture. Pipe defects can occur during installation, routine maintenance excavations, or new civil engineering work near the pipes [4]. For example, during pipe maintenance operations, mechanical damage may occur as a result of negligence, clumsiness or a lack of precautions. If site workers are unable to precisely locate the buried pipe, this structure may be subjected to shock by a tool like bucket teeth or construction machine. Most of the time, the incident goes unnoticed or unreported.

Mechanical interference caused by foreign object contact accounts for approximately 50% of pipeline damage in Europe and 53.5% in the US [5]. This confirms that external damage causes the vast majority of pipeline ruptures, whether on land or at sea. These flaws can take the form of dents, cracks, or a combination of the two [6]. The structural damage induced by the presence of these deficiencies can be exacerbated if the pipeline is subjected to internal pressure of variable amplitude loading, such as water hammer waves [7]. In fact, transient flows in the pipeline network can be created by pump failure, pipe rupture, or a sudden change in the state of the valve that controls the flow of fluid through the pipeline. This can cause a pressure pulse to travel at high speeds along the pipeline in the form of a pressure wave, causing vibrations that can eventually burst the pipe [8].

The industrialists who specializes in the area of piping networks are concerned about the safety of the population as well as the environment, given the impact that a major failure can have, especially in the case of flammable gases or explosives [9]. Besides that, economic and financial aspects must be considered, as financial losses in terms of public works, pipe replacement, and operating losses are substantial. Thus, breakage prevention is critical, and it is achieved through inspection and analysis of the harmfulness of discovered defects [10, 11]. This analysis necessitates the use of specialized tools in order to assess the potential damage caused by a defect in an internally pressurized pipe.

There are several methods in the literature for determining the severity of a crack, dent, notch, or corrosion defect in a pipeline [9-14]. They are frequently developed using limit analysis, fracture mechanics, and notch fracture mechanics. Depending on the type of defect, the appropriate tool is selected. The limit analysis is frequently used to assess defects such as corrosion or dents [9]. In the case of defects such as weld cracks, sharp notches, or a combination of a dent and a notch, a mechanical fracture approach is preferable.

*CORRESPONDING AUTHOR | Zakaria Mighouar | ✉ z.mighouar@gmail.com

Dented and cracked pipes in the presence or absence of internal pressure have been studied in recent years in terms of the risks they pose, using various approaches: theoretical, experimental, or numerical [4-6, 9-15]. In the literature, there is still a lack of a model that can be adapted to different types of defects. Furthermore, the majority of these studies do not account for the dynamic effect of loading. However, it has been demonstrated that this effect has an impact on the defect's harmfulness and is to be considered if precise results are sought [16]. The research presented in this paper is focused on mechanical damage defects, and more specifically to smooth dents and surface semi-elliptical cracks.

Previous research by the authors allowed for the development of finite element models [17, 18] that were tailored to each defect category studied (one for cracked pipes and one for dented pipes). The stress intensity factor (SIF) along the crack front is calculated using a cracked pipe numerical model. The stress concentration factor (SCF) near the dent defect is calculated using a dented pipe model. These parameters allow the harmfulness of a defect in a metal tube under internal pressure to be evaluated. Each model was used in a separate study to compare and classify defects of various categories (e.g., dent and crack) based on their nocivity.

Since the tools used to classify crack defects differ from those used to classify dent defects, it has been impossible to directly compare defects from these two categories. As a result, the authors [19, 20] developed a numerical damage assessment model that uses the results of these two finite element models to assess damage accumulation in the defected pipeline. This dimensionless parameter will make it possible to compare the harmfulness of various defect categories on the same scale. Analytical models were developed and correlated with results from the finite element models in the previous studies. The obtained models are then validated in order to replace the numerical calculation, as they produce nearly identical results in terms of SIF for cracked pipes and SCF for dented pipes. These analytical models are used in a numerical damage accumulation model developed in Scilab, which takes into account the interaction effect and the loading history. This model is developed to evaluate the severity of a pipeline defect caused by each loading cycle. This paper provides a brief overview of the various models. Details on the development and validation of these models can be found in [19, 20].

The damage assessment model takes as input history of pressure peaks caused by a sudden change in flow velocity. The characteristic method is used to solve the transient flow equations in the pipe to generate this pressure spectrum. More information on the calculation process can be found in [16]. Based on an appropriate fatigue life estimation model, the damage is estimated for each pressure cycle. In the case of dented pipes, fatigue life is derived from SCF and loading parameters; in the case of cracked pipes, fatigue life is derived from SIF and loading parameters. The accumulation damage model is validated against published experimental data in the literature for each defect category. This model is used in this paper to reach conclusions on key parameters that affect the severity of the studied defects, as well as to compare and classify the different types of dent defects with the different types of crack defects present in a pipe subject to variable amplitude loading. This will allow for the identification of equivalence between several types and categories of defects in terms of structural damage.

This paper focuses on the investigation of defective pipes that have been subjected to water hammer waves as a result of a sudden change in valve status (fast closing or opening) or even a pump failure. The effects of the loading sequence and the loading history are considered in this study. The considered semi-elliptical cracks are internal and external surface cracks located in the base material of the pipe, in the welding bead or the heat-affected zone (HAZ). The dents investigated are of various shapes (spherical and rectangular) and orientations (longitudinal and transverse) in two configurations (constrained and unconstrained). The following section explains the distinction between constrained and unconstrained denting.

FINITE ELEMENT MODELS

Dent Defects

In some cases, when a foreign body collides with a pipe, the cross-section of the pipe wall experiences irreversible plastic deformation known as a dent [21]. Dents can produce stress concentration in the pipe, making the structure more vulnerable to fatigue damage caused by internal pressurization. The geometric parameters of the dent defect are shown in Figure 1. A dent can be characterized more precisely in terms of its capacity to move following internal pressure, i.e., unconstrained dents can re-round under pressure while constrained dents cannot. A constrained indentation is defined in general by the presence of a retaining object, usually the indenter [5].

During construction, laying the pipe on a stone or rock might also result in a constrained dent. According to Rosenfeld [22], it is conceivable for excavating equipment to generate dents at the bottom line of small diameter pipes. Furthermore, it is likely that local restraint in the vicinity of the dent caused by wall thickness or the nature of the dent prevents it from responding to pressure fluctuations. These indentations are also known as restrained dents, and this term is used in other parts of the literature [22]. The broadest definition of the constrained dent was employed in this work to define any dent that is not able to re-round when the structure is subjected to internal pressure. Cracks are initiated and propagated in the vicinity of the dent where the stress concentration is highest due to the action of cyclic internal pressure, resulting in material fatigue. It is consequently critical to be able to forecast the fatigue life of a dented pipe in order to anticipate and thus avoid structural failure.

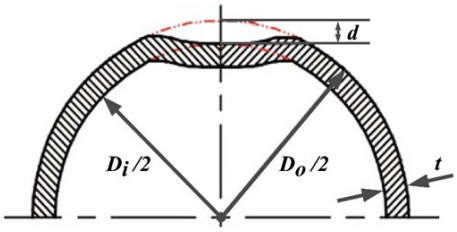

Figure 1. Dent defect parameters.

Several authors [1, 2, 5, 6, 14, 22] have explored the fatigue behavior of pipes with a wide range of diameters and wall thicknesses indented to varying depths. Furthermore, a substantial amount of study has been conducted to understand the effect of different forms and sizes of indentations on the behavior of pipelines under static and cyclic pressures [13, 17, 23]. Design fatigue curves have been used to construct a range of semi-empirical and empirical models for estimating dent fatigue life. The main concept is to use published fatigue curves (S-N) from a relevant design code [5, 21-26] and account for stress concentration caused by the dent with the stress concentration factor. It should be emphasized that this method implies that there are no initial cracks in the dent, therefore fatigue life includes the duration required to initiate and propagate a crack [5].

In addition, there is no standard for calculating the stress concentration factor. Some authors [23, 26] employed experimental determination, whereas others [1, 6, 13, 17, 22] used finite element modeling. The disadvantage of utilizing FEM to derive stress concentration factor is that a complete examination of each indentation to be investigated is required, which is an expensive and time-demanding operation. Some authors, including the paper's authors [20, 27, 28], attempted to establish an analytical equation based on FEM data to relate the SCF to the geometry of the dent. These formulae can be used to calculate the stress concentration factor under static or cyclic load for a wide variety of dent and pipe diameter values.

Cunha et al. [13] used published experimental data to compare the available methodologies for evaluating dent fatigue. This study advises using the Petrobras model [29] in Eq. (1) because it offers the greatest match to the test data due to the fact that it accounts for the effect of the mean stress. The S-N curve is derived for given mean stress and is modified by the SCF caused by a dent in a metal pipe.

$$N = \left[\sigma_A \Big/ \sigma_F \left(1 - \left(\frac{\sigma_M}{UTS} \right)^2 \right) \right]^{\frac{1}{b}} \text{ for N<}10^6 \text{ cycles} \tag{1}$$

$$b = \frac{1}{6} \log_{10} \left(\frac{0.325 \times UTS}{\sigma_F \times SCF} \right) \tag{2}$$

where σ_A is the alternating stress, σ_M is the mean stress, σ_F is the true stress of failure, and UTS is the ultimate tensile strength.

This model is the one used in our research to estimate the fatigue life of pipes with dents of several dimensions, shapes, orientations, and configurations. The stress concentration factor in Equation 2 is calculated using a previously developed FEM of a dented pipe. This numerical model provides the SCF from the Von Mises stress measured around three types of indentations (spherical, longitudinal rectangular and transverse rectangular) in two configurations (constrained and unconstrained). The finite element model is developed using the ANSYS code. A validation study revealed that this model can accurately provide the stress concentration factor in the case of a dented pipe. Using the Petrobras model [29], one can derive the S-N curves for the indented pipe using this factor. The analyzed pipes are built of API 5L X52 and have an external diameter of 274 mm, a length of 1100 mm, and a thickness of 13.7 mm. The reason for selecting this material is that existing pipelines, which are the most prone to defects, are primarily composed of it. The dimensions chosen in our study represent those of an average pipeline; they were also chosen in order to be able to calibrate and validate our finite element model of a dented pipe with experimental work conducted by CERP [30].

It should be noted that, as with most FEM software, it is highly preferable that the stress-strain data entered into ANSYS be true stress-strain data. Rather than the material's initial undeformed state, these curves correlate the current deformed state with the history of previously performed states. The use of the true stress-strain curve is also due to the fact that the resulting curve is an increasing function and thus associates a single strain value to stress in the plastic field, as opposed to stress-strain-engineering curves, which may associate two strain values with one stress value, causing program confusion. The hardening law adopted for the analysis of nonlinear finite elements is that of isotropic hardening with as data, the true stress-strain curve of the material (Figure 2). These data are obtained by converting the experimental data of engineering stress-strain provided by the CERP using Eq. (3) and Eq. (4). Table 1 summarizes the mechanical parameters of the material required for our study.

$$\sigma_{true} = \sigma_{engineering} \times \left(1 + \varepsilon_{engineering} \right) \tag{3}$$

$$\varepsilon_{true} = ln\left(1+\varepsilon_{engineering}\right) \tag{4}$$

where σ_{true} is the true stress, $\sigma_{engineering}$ is the engineering stress, ε_{true} is the true strain, and $\varepsilon_{engineering}$ is the engineering strain.

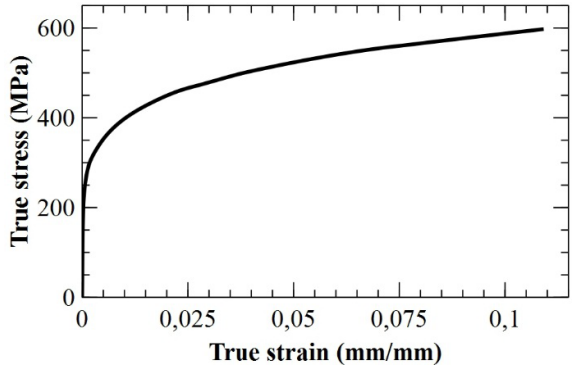

Figure 2. True stress-strain curve of the API X52 material.

Table 1. Mechanical properties of API X52 material.

Young's Modulus, E	Poisson's ratio, υ	Yield strength, σ_E	Ultimate tensile strength, UTS	True stress of failure, σ_F
200 GPa	0.3	410 MPa	498 MPa	579 MPa

A spherical indenter with a diameter of 50 mm and a rectangular indenter with a base of 100.34×19.28 mm are used to simulate the indentations. The rectangular indenter is about the size of an excavating bucket's tooth. The dimensions of the spherical indenter allow the simulation of a stone being pushed up against the wall of a pipeline.

The longitudinal and transverse indentations are produced by altering the orientation of the rectangular indenter. The indenters are assumed to be infinitely rigid and to be in frictionless contact with the pipe's outer surface. To reduce simulation computation time, the numerical model is reduced to one-quarter of the pipe and indenter. Figure 3 shows the boundary conditions employed in this FEM.

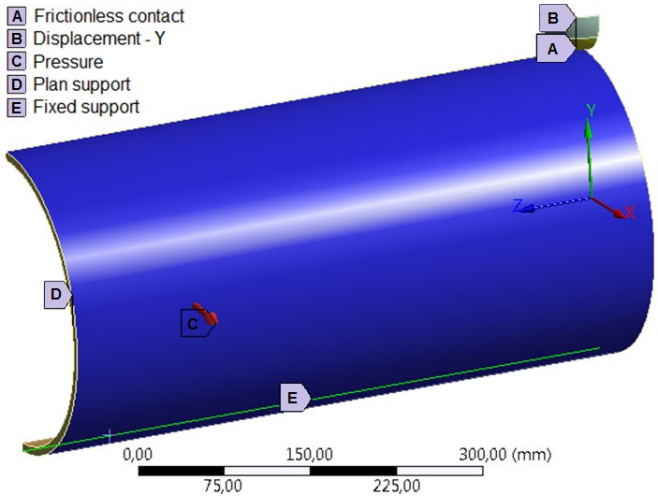

Figure 3. Boundary conditions of the finite element model of a dented pipe.

The mesh of the finite element model is refined to 5 mm at the area to be indented and exhibits a transition on the size ratio of 10 in the longitudinal direction from the middle of the pipe to its end. The mesh is created using 8 hexahedron nodes with 6 degrees of freedom. The pipe and indenter mesh is made up of 22176 nodes and 4484 elements.

An internal pressure cycle is applied to the inner surface of the dented pipe model. This allows us to utilize Eq. (5) to calculate the stress concentration factor by measuring the maximum Von Mises stress surrounding the dent numerically. The research in [17] covers details on the model's development as well as the validation study.

$$SCF = \frac{\sigma_{MAX}}{\sigma_{NOM}} \tag{5}$$

$$\sigma_{NOM} = \frac{pD_i}{2t} \tag{6}$$

where σ_{MAX} is the maximum equivalent stress measured by finite element analysis, σ_{NOM} is the nominal stress, and p is the internal pressure of the pipe.

The results of this finite element model are utilized to develop an analytical model for computing the SCF. This analytical model is then employed in a numerical model for determining the accumulation of damage caused by the presence of a dent in a pipe subjected to variable amplitude loading.

Crack Defects

Weld and crack flaws may be classified as design, manufacturing, or construction defects according to the abnormalities discovered during the inspection. The faults seen in welded joints are commonly classified as semi-elliptical cracks [6], such as those caused by a lack of weld material penetration or a defect in the shape of the weld bead. Having stated that, mechanical interference is responsible for the vast majority of cracks [5]. Figure 4 depicts the parameters of a semi-elliptical crack.

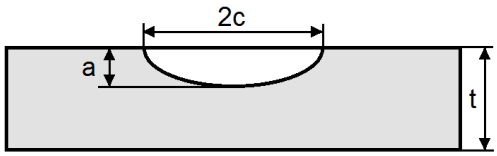

Figure 4. Surface crack parameters.

Surface cracks manifest as a local separation of two surfaces known as lips; various investigations have been undertaken to establish the root causes of this type of defect [31]. According to those studies, cracks caused by the welding process may appear on the weld metal (WM) or in the heat-affected zone (HAZ). Cracks can arise in either of these two regions or in the pipe's base material (BM) as a result of external or internal mechanical interference. This type of defect can also form during solidification or after a prolonged welding operation [31]. In fact, microcracks begin to appear in the material and propagate at an increasing rate. Failure occurs when the residual thickness of the wall near the crack no longer allows the structure to withstand the applied stress. This failure occurs only when a sufficient number of load cycles have been applied to expand the initial crack.

Understanding fatigue failure requires an understanding of fracture mechanics theory. Fracture mechanics predicts the macroscopic mechanical failure of structures by applying theories of elasticity and plasticity to microscopic flaws observed in materials [32]. There are two major branches of fracture mechanics [32]; elastic-plastic fracture mechanics (EPFM) and linear elastic fracture mechanics (LEFM). The LEFM is a method for studying cracked solids that assumes the material is linear elastic and isotropic. Because it is the foundation upon which the other fracture mechanics theories are established, the LEFM represents the majority of practical uses of fracture mechanics. The LEFM employs two approaches; energy calculations and stress intensity calculations. The stress intensity approach is the most often utilized since it exploits the stress and strain distributions surrounding the crack directly, which is typical in industrial applications. The range of stress intensity parameters derived as a function of crack geometry and structure loading, according to LEFM, unequivocally characterizes crack propagation [33].

The literature contains detailed descriptions of structures subjected to constant amplitude loads. However, studies on fracture damage induced by variable amplitude that have been published in the literature still require additional development since they are more complex and depend on the load history [32]. Paris et al. [34] assumed that crack propagation under varying loads would follow the law, commonly referred to as the Paris' law. This is the first relation that describes the behavior of crack growth. Several studies [16, 33, 35, 36] later improved on this rule by incorporating correction coefficients to account for other aspects such as the geometry of the structure, the position and shape of the surface crack, or the crack closure effect.

Elber [35] discovered the phenomena of crack closing during experimental tests. This phenomenon happens during a load cycle involving two loading values (i.e., a minimum value of stress cycle, K_{MIN}, and a maximum value of stress cycle, K_{MAX}), when the crack begins to close prior to the stress intensity factor reaching K_{MIN} as a result of contact between the crack surfaces. The crack appears to cease closing at a magnitude of the stress intensity known as K_{OP}, which it opens at. Elber [35] proposes and incorporates an effective stress intensity range, ΔK_{eff}, into the Paris law. This factor is based on the assumption that the process phase below K_{OP} does not contribute to the growth of fatigue cracks owing that to the closure effect. This crack closure effect slows the spread of fatigue cracks.

A modified Paris model is utilized in this study to predict the number of cycles to fatigue, N, in the case of a cracked pipe. This can be stated in the form of Eq. (7), taking into consideration the effect of crack closure and some rearrangement.

$$\frac{da}{dN} = C\,\Delta K_{eff}{}^{m} = C\left(0.25\,K_{MAX} + 0.5\,K_{MIN} + 0.25\frac{K_{MIN}{}^{2}}{K_{MAX}}\right)^{m} \tag{7}$$

where C and m are the material constants of Paris' law.

In a prior study, the authors [19] developed and validated a finite element model of a cracked pipe. Using the ANSYS calculation code, this model enables to calculate the effective stress intensity factor induced by semi-elliptical cracks of various orientations (longitudinal and transverse) and positions (external and internal). These cracks can be found in the three materials that make up a longitudinally welded pipe (base metal (BM), weld metal (WM), and heat-affected zone material (HAZ).

The stress intensity factor is determined at the crack front. The acquired results are utilized to estimate the number of cycles that cause the structure to rupture. The longitudinally welded pipe used in the FEM has the same dimensions as the one used in the dented pipe analysis. Table 2 presents the mechanical parameters of each of the three zones. Figure 5 depicts the numerical model's boundary conditions. Unlike in the dented pipe analysis, the geometry for the FEM of a cracked pipe was not limited to a quarter of a pipe. This is primarily due to the fact that the semi-elliptical crack is embedded with an ANSYS functionality that requires the material of the structures to be visualized.

The pipe mesh is refined using a sphere of influence to improve the mesh around the crack, with an element size of 0.6 mm and a diameter of $1.2 \times c$. To enhance the convergence of the circumferential stress, the mesh is refined on the circumferential zone encompassing the crack. It should be noted that the results of this FEM are utilized to develop an analytical model for computing the SIF. This analytical model is then employed in a numerical model to calculate the accumulation of damage caused by a crack in a pipe subjected to varying amplitude loads.

Table 2. Material properties of three zones of the longitudinally welded pipe.

Material	Paris' law material constants		Critical fracture toughness
	C	m	K_{IC} (MPa.m$^{0.5}$)
Base metal	3.3 e^{-09}	2.74	53.36
HAZ	1.13 e^{-09}	3.25	53.36
Weld metal	1.04 e^{-09}	3.28	61.02

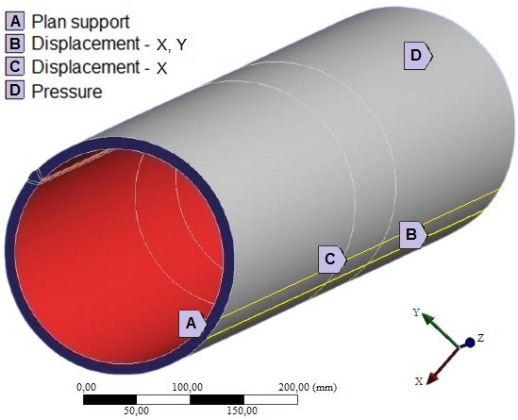

Figure 5. Boundary conditions of the finite element model of a cracked pipe.

ANALYTICAL MODELS

Dent Defects

According to the literature, the stress concentration factor is directly influenced by the geometry of the component, with no relevance to material qualities [37]. Two non-dimensional characteristics were discovered to be responsible for the stress concentration generated by the presence of a smooth dent. These parameters are the outer diameter to pipe thickness ratio, D_o/t, and the width of the dent to pipe outer diameter ratio, d/D_o.

A mathematical formulation of the stress concentration factor can be developed based on the data obtained from the developed finite element model. The SCF calculation formula can be written as a power function in terms of pipe and dent geometry for numerous types of dent defects [38]. This formula is detailed in Eq. (8).

$$SCF = 1 + A\left(\frac{D_o}{t}\right)^B \left(\frac{d}{D_o}\right)^C \tag{8}$$

The coefficients A, B, and C of the SCF equation are adjusted to ensure the best possible match with the numerical data achieved from the developed finite element model. The interpolation coefficients were derived through nonlinear fitting of the appropriate numerical data in [20]. Table 3 lists the dimensionless coefficients for each type of dent.

The mathematical equation's results deviated only slightly from those of the finite element model [20]. The stress concentration factor of the dented pipes can then be calculated using the previously established equation. The purpose of

developing this equation is to use it in an algorithm to calculate the damage accumulation induced by a pressure cycle on a dented pipe.

Table 3. Interpolation coefficients used for the calculation of the SCF by type and configuration of the dent [20].

	Dent type	Spherical	Rectangular longitudinal	Rectangular transverse
		Unconstrained dents		
Coefficient	A	1.483	13.667	1.235
	B	0.590	0.800	0.984
	C	0.541	1.097	0.850
		Constrained dents		
	A	0.426	2.711	0.284
	B	0.638	0.893	1.097
	C	0.228	0.818	0.644

Crack Defects

Many researchers have been interested in using various approaches to determine the harmfulness of cracking defects in pressurized structures [6, 11, 32, 33, 36, 39]. This is due to the fact that the rupture or leakage of these structures poses a serious risk. The approaches based on the stress intensity factor are the most extensively employed, whether in scientific research or industry. The first models that have emerged deal with the case of an infinitely large plate subjected to uniaxial loading [40]. Several researchers [41, 42] have agreed that Newman's model provides the best estimates of the stress intensity factor for the case of a surface crack. Several studies have been devoted to the development of correction factors based on this same model and in order to generalize it to other cases of structures. The most important are those that take plate thickness, structure curvature, and the plastic zone at the crack tip into account [33, 43].

In our case, as with the other researchers, there was a need to improve the convergence of this analytical model for high pressures and to account for the position of the crack in relation to the wall (internal and external). The reason for this choice is that industrialists do not follow the recommendations emitted by the organisms operating in the field to the letter and tend to increase the pressures to the recommended limit. As a result, this study attempt to investigate the structure's behavior when pressures are very high.

To accomplish this goal, a correction coefficient (f_1+a^{f2}) has been proposed and calibrated based on a previously developed and validated finite element model of a cracked tube [16]. Equation (9) depicts the modified Raju and Newman model with multiple correction coefficients. Equations (10) to (14) show the various terms involved in this model. The f_1 and f_2 factors are tweaked to produce the best possible concordance with numerical findings from the established finite element model. Table 4 displays the coefficients of the correction factor used in the SIF equation for each crack position.

$$K_I = \left(f_1 + a^{f2}\right) \cdot k_1 \, p\sqrt{a}\, M_{TM} \left(1 + k_2\, a^s\right) \tag{9}$$

where M_{TM}, k_1, k_2, k_3, and s are correction factors defined as :

$$M_{TM} = \left(1 - \frac{a}{t}\right)^{-1} \times \left(1 - \left(\frac{a}{t}\right) \Big/ \sqrt{1 + \frac{6.4\ c^2}{\left(D_i + D_O\right) \times t}}\right) \tag{10}$$

$$k_1 = k_3 \times \frac{\sqrt{\pi}\, D_i}{2 \times t} \tag{11}$$

$$k_2 = \frac{t^{-s}}{k_3} \times \sqrt{\frac{c}{a}} - 1 \tag{12}$$

$$k_3 = \left(1.13 - 0.1 \times \frac{a}{c}\right) \Big/ \left(1 + 1.464 \left(\frac{a}{c}\right)^{1.65}\right) \tag{13}$$

$$s = 2 + 8 \left(\frac{a}{c}\right)^3 \tag{14}$$

The resulting analytical model produces findings that are quite close to those of the FEM one and can thus be used to determine the stress intensity factor to predict the fatigue life of a cracked pipe [16]. This model is later employed in this study in a numerical model of damage accumulation.

Table 4: Interpolation coefficients used for the calculation of the SIF by the position of the crack [16].

Coefficient	Crack position	
	External	Internal
f_1	-0.056	0.0447
f_2	0.052	0.00188

DAMAGE ACCUMULATION MODEL

Throughout the operation, the internal loading of pipeline transmission lines varies, causing structural fatigue. Thus, the material of the pipeline undergoes alterations, resulting in fatigue damage [44-45]. As a result, developing models that explicitly account for fatigue loading variability is critical for researchers [12]. The authors suggested a nonlinear model for fatigue damage accumulation [19]. To assess the damage induced for each loading cycle, the fatigue life prediction models employed in the cracking and denting situations are operated separately based on a modified Miner's law. The algorithm for this numerical model, depicted in Figure 6, is based on the work of Thun et al. [46]. The effects of load interaction and load history are considered in this model. It is capable of calculating cumulative damage under variable amplitude loading levels. The leakage or collapse of the structure may be expected when the cumulative damage reaches a critical value (equivalent to unity in our study).

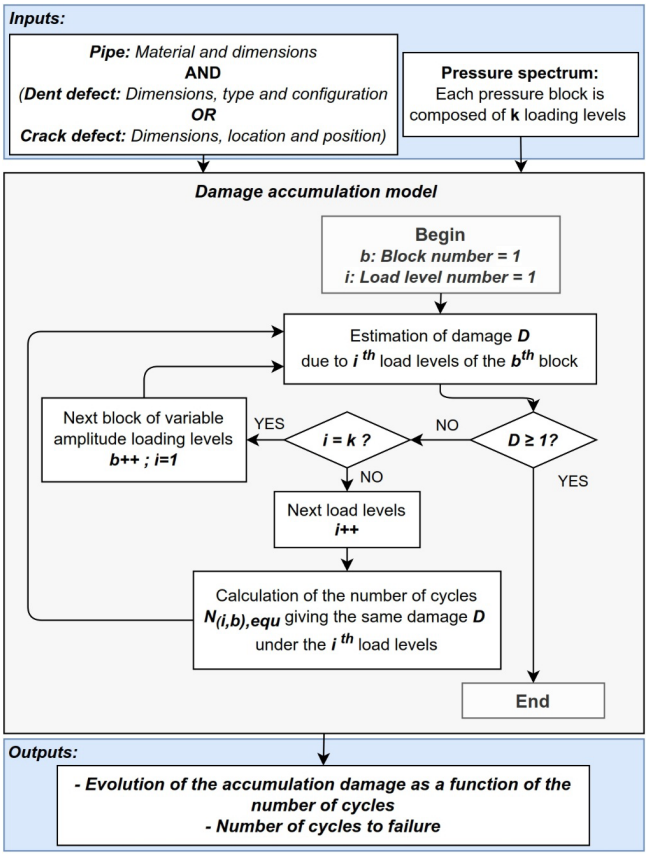

Figure 6. Nonlinear damage accumulation model algorithm.

In the instance of cracked or dented pipes, this damage accumulation model can be used to determine the nocivity of the defect. The dent depth, d/D_o, and material endurance limit, σ_D, are employed as supplementary parameters in the dent case fatigue life prediction model. If the analyzed defect is a crack, the model for calculating fatigue life includes as added parameters the crack dimension, a/c, the constants of Paris' law, C and m, and the critical stress intensity factor, K_{IC}. The pipe, as shown in Figure 7, is assumed to be subjected to variable amplitude internal pressure. The water hammer phenomenon causes those pressure peaks, which arise as a result of an abrupt shift in the valve state (opening/closing) that controls the flow of fluid in the pipeline. This trace of pressure history is generated using the method of characteristics to the transient flow equations in the pipe [16].

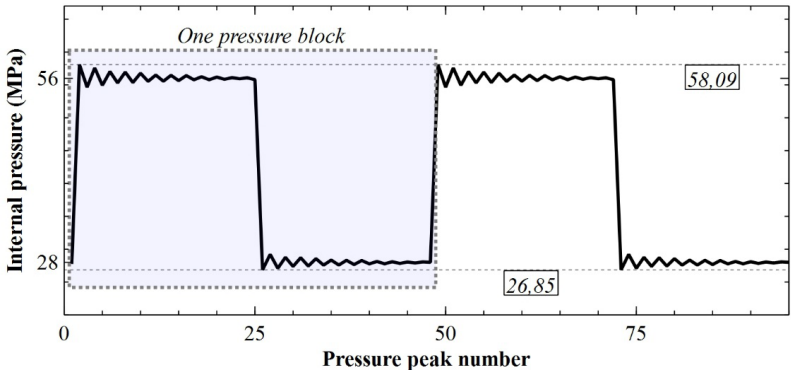

Figure 7. Internal variable amplitude loading of the pipe caused by the water hammer phenomenon.

Only two pressure blocks are depicted in Figure 7. However, this pressure spectrum will be applied to the structure until the critical value of the damage is reached in order to estimate the number of blocks (number of cycles) until failure. To simulate the new trends in industrial pressurization, the two values around which the pressure switches are moderate pressure and high internal pressure. Figure 8 depicts the stress ratio and amplitude ratio as a function of cycle number to better visualize the loading conditions experienced by the pipeline. It's worth noting that this is only for a single pressure block.

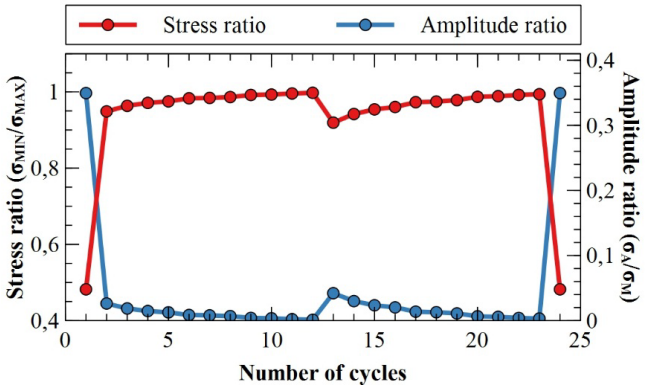

Figure 8. Stress and amplitude ratios of pipe loading caused by a single pressure block of the water hammer phenomenon.

PARAMETRIC ANALYSIS

The analysis performed in this paper is divided into different phases. During the first phase, 144 cases were investigated to determine the effect of water hammer waves on the severity of a semi-elliptical crack present in a metal pipe. The dent defect is the focus of the second phase, which includes 48 cases. During these two phases, the same numerical model will be used to estimate the accumulation of damage in the pipe. The calculation formulas used by this model are tailored to the type of defect (crack or dent). Throughout the crack and dent studies, as well as during the water hammer analysis, the pipe's material and dimensions are kept the same. The goal of this last analysis is to estimate the pressure waves induced by the water hammer phenomenon, which is caused by a sudden change in the state of a valve of a pipe transmission line carrying water. The obtained pressure spectrum presented in Figure 7 is used as input in the proposed damage accumulation model (Figure 6). The D_o/t ratio of the studied pipe is 20.

The dent depth parameter, d/D_o, is considered in the dent defect analysis with the following values: 0.025, 0.05, 0.075, 0.1, 0.125, 0.15, 0.175, and 0.2. The dent types are spherical, longitudinal rectangular, and transverse rectangular. The impact of the dent's configuration (constrained or unconstrained) is also being investigated. The crack defect under investigation is a semi-elliptical surface crack. During the crack defect assessment, the initial crack depth is assumed to be 0.5, 1, 1.5 and 2mm. The crack dimensions, a/c, considered are 0.4, 0.5, 0.6, 0.7, 0.8, and 0.9. The crack is assumed to be in the base metal, weld metal, or heat-affected zone. The location of the crack (whether external or internal) is also investigated.

RESULTS AND DISCUSSION

The presence of several types of defects in a metal pipe is analyzed using the validated damage accumulation model. The obtained results are depicted in the form of figures. Figure 9 shows the evolution of the accumulation of damage for a dented pipe subjected to water hammer pressure waves. These curves will lead to assessing the effect of the dent's depth, shape, orientation, and configuration on the evolution of the accumulation of damage until the structure collapses. The rupture of the structure is predicted if the damage accumulation is equal to unity. Figures 10 to 13 show the results of the evolution of damage accumulation in a longitudinally welded pipe with a crack. This pipe is subjected to variable

amplitude internal pressure, similar to the dented pipes. The main objective of these figures is to examine the effect of crack size, location, and initial depth on the evolution of accumulation damage up to structural failure.

A common scale is used on the axis of the number of cycles in Figure 10 to 13. This allows for a visual comparison of the effect of the crack's location on the evolution of the damage. This was not possible for the figures dealing with dented pipes due to the large differences in the term of the number of fatigue cycles. To improve the readability of those results, the axes of the number of cycles in fatigue for the spherical and transverse rectangular indentations are on the same scale, and on a scale with a factor of 10 for the longitudinal rectangular indentations. A comparative study is carried out with the goal of classifying the various cases studied in terms of their harmfulness. Figure 14 and 15 depict the study's findings.

Figure 9 shows the fatigue life values of 634261, 277750, and 52173 for spherical, rectangular transverse, and rectangular longitudinal dents, respectively, for an unconstrained dent of 2.5% depth. The fatigue life values of 576243, 364870, and 56562 for spherical, transverse rectangular, and longitudinal rectangular indentations, respectively, can be read from Figure 9 for a constrained dent of similar depth. The fatigue lifetimes for unconstrained dents in a rectangular shape are less than those for dents of the same shape in a constrained configuration, as can be seen from these results. The opposite is true for the 2.5% depth spherical dent, but this is the only case in question. This case confirms the experimental finding by Alexander [23] that for small dent depths and especially for spherical or quasi-spherical shapes, constrained dents have shorter lifetimes than unconstrained dents of the same size. Having said that, the authors are more focused in this research on dents with a consequent depth, which pose a greater risk to the structures of fluid transport under pressure. However, this could be a very interesting avenue for better understanding the mechanisms underlying the harmfulness of dented defects, and it should be addressed in future studies to improve the numerical model results.

As a result, except for the dents with depths of 2.5%, all of the other unconstrained cases studied have a shorter fatigue life than the constrained dents with the same depth and shape. As a result, it's deduced that unconstrained dents are more harmful than constrained dents. This is explained by the fact that, in the case of constrained smooth indentations, the indenter rests on the exterior surface of the pipe and serves as an extra boundary condition, reinforcing the structure and reducing the indentation's potential deformations. It should be noted, however, that in the case of extremely high pressure, the pipe wall will compress at the level of the indentation.

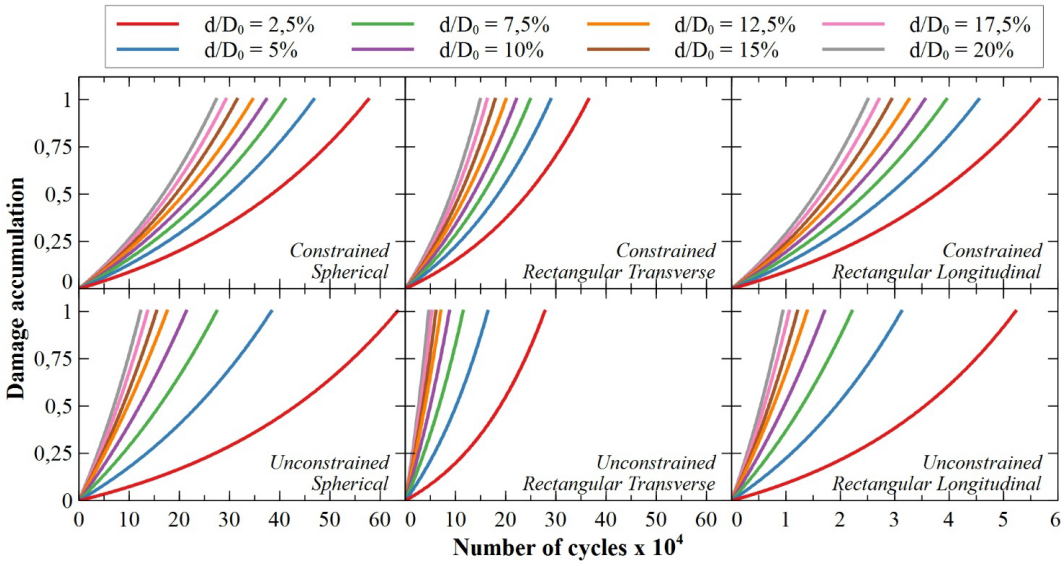

Figure 9. Effect of the dent configuration, type and depth on fatigue accumulation damage.

For a pipe with a dent having a depth, d/D_o, of 10%, there is a deviation of -58.9 and -92.02% for the transverse and longitudinal dent, respectively, compared to the result obtained in terms of fatigue life for an unconstrained spherical dent. For a constrained dent of the same depth, a deviation of -40.82 and -90.47% is observed with respect to a spherical dent for the transverse and longitudinal dent, respectively. These deviations show that the effect of the dent's shape and orientation is very important and should not be overlooked during the assessment of the harmfulness of dent defect in a pipe. It is also safe to conclude that the rectangular dent is more harmful than the spherical dent and that this harmfulness is exacerbated by the effect of the orientation when it shifts from transverse to longitudinal. This observation holds true regardless of the depth or shape of the dent.

To better understand the effect of dent depth on the fatigue resistance of a dented pipe, and to calculate the deviations between the values of the number of fatigue cycles (corresponding to a value of accumulation of damage, D, of 1), let us use the value obtained for an immediately greater dent depth as a reference. This is equivalent to comparing the result obtained for a dent depth of 10% to that obtained for a dent depth of 12.5%.

For the cases of unconstrained spherical indentations, one can notices a relative deviation of -18.83, -12.31, -9.07, -7.34, -8.88, -7.09 and -6.56% for the dent depths, d/D_o, of 5, 7.5, 10, 12.5, 15, 17.5 and 20% respectively. For the dents of the same shape in the constrained configuration, a deviation of -39.65, -28.4, -21.99, -17.95, -11.98, -11.28 and -9.78%

is observed for the dent depths of 5, 7.5, 10, 12.5, 15, 17.5 and 20% respectively. Based on these deviations, it can be confirmed that the greater the dent depth, the more the fatigue life decreases. It is also observed that this increase in depth has less and less effect on the fatigue strength of the dented pipe. This observation is valid regardless of the shape and configuration of the dent.

It's worth noting that the first loading cycle causes very negligible damage, but is not equal to zero. It is of the order of magnitude 10^{-4} in all cases of dented pipes. This does not apply to the case of cracked pipes. In fact, one can see from Figure 10 to 13 that the damage caused by the first pressure cycle of 0.036, 0.073, 0.109, 0.146 and 0.182, which is caused by the presence of a crack of an initial depth of 0.5, 1, 1.5, 2 and 2.5 mm. These damage values correspond to the initial depth of the crack divided by the thickness of the pipe. For example, the value of damage of the first cycle for a pipe with an initial crack of 0.5 is of (0.5 mm /13.7 mm) which is equal to 0.036. This is due to the fact that the damage estimation model takes the maximum value between the ratios a/t, and K_I/K_{IC} for each pressure cycle. This reveals that for all of the cases of cracked pipes studied in this paper and for the first peak of the pressure spectrum, we obtain a value of a_{ini}/t, greater than K_I/K_{IC}.

Consider the case shown in Figure 10 of a pipe with a 0.5 mm initial depth crack located at the HAZ. When the result, in terms of the number of cycle to fatigue, obtained for each dimension of crack, a/c, is compared to the result obtained for the immediately lower dimension, a variation of 177, 71.98, 56.6, 42.26, and 38.76% is found for the external cracks of dimensions 0.5, 0.6, 0.7, 0.8, and 0.9, respectively. Results obtained for pipes with internal cracks with similar locations and dimensions have a deviation of 176.6, 71.87, 56.51, 42.2 and 38.72%, respectively, for cracks with dimensions 0.5, 0.6, 0.7, 0.8, and 0.9. It is clear from these deviations that the effect of the crack dimension on fatigue life decreases as a/c increases. It is also noted that the deviations obtained for internal cracks are nearly identical to those obtained for external cracks. This means that regardless of the position of the crack, the effect of the parameter a/c on the harmfulness of the crack defect is the same. This observation holds true regardless of the localization of the crack (BM, WM, or HAZ) or the initial depth of the crack. It can also be concluded that the crack defect is more harmful at low a/c values.

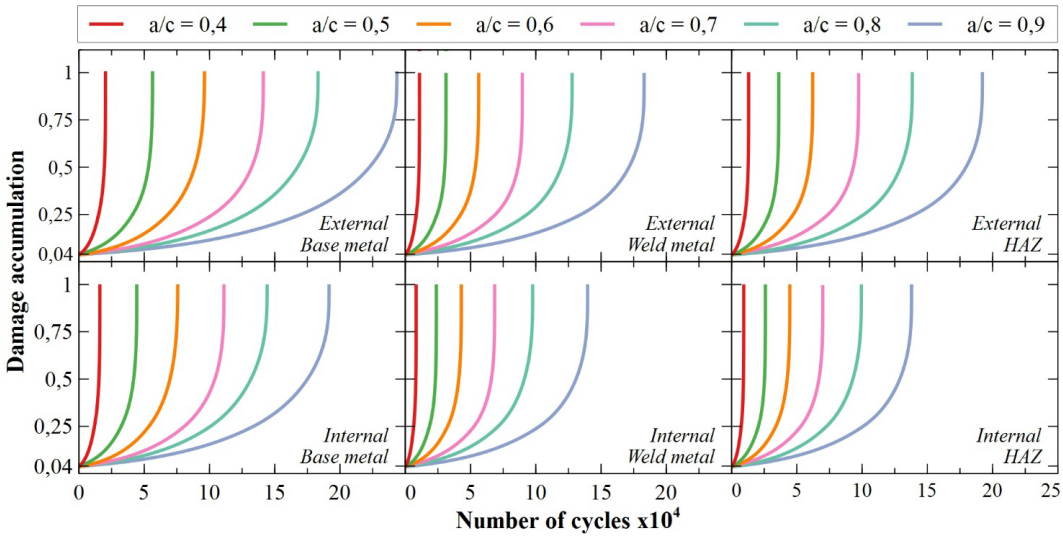

Figure 10. Effect of surface crack with an initial crack depth of 0.5mm on fatigue accumulation damage.

From Figure 11, let us consider the case of a crack with an initial depth of 1 mm and dimensions $a/c = 0.6$, and use the values in terms of life in fatigue obtained for pipes with external surface cracks as a reference for calculating the deviations. There is a difference in the results for the external and internal cracks of -21.33, -23.67, and 28.21% for cracks located at the base metal, weld metal, and heat-affected-zone. On the one hand, these deviations indicate that internal cracks are more harmful than external cracks of the same dimensions. On the other hand, the effect of the crack's location becomes even more pronounced when the crack is located in the HAZ. This is true regardless of the initial depth and a/c dimensions of the semi-elliptical surface crack.

Figure 11 shows that for cracks $a/c = 0.6$ with an initial depth of 1 mm, the fatigue life of -39.56 and -34.29% decreases when external cracks located in WM and HAZ are compared to the results obtained for a localized crack in the BM. When comparing the internal cracks in the WM and HAZ to the cracks in the BM, one notices a deviation of -41.35 and -40.04%. Based on these deviations, it can be concluded that the crack is more harmful when it is located in the WM. It should also be noted that the consequence of a crack defect located in the WM or HAZ is very similar, especially when compared to the same crack located in the BM.

The microstructure of the weld at the joint is influenced by the welding technique, bead design, duration of weld passes, heat input, and other parameters. This, in consequence, influences the extent of the HAZ and residual stresses that accumulate in the structure's base metal. These factors impair fatigue strength by increasing the likelihood of crack nucleation and early development, which will lead to pipeline collapse. Thus, the microstructural alterations have a significant impact on the fatigue crack development capabilities of each material that makes up the longitudinally welded pipe. According to the conclusions of this and previous investigations, the HAZ is the most impacted zone.

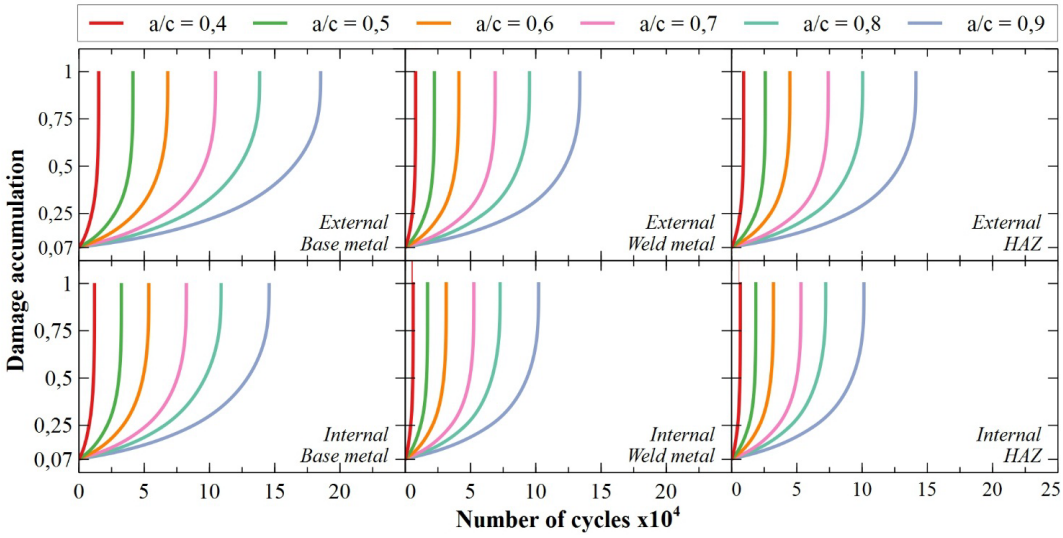

Figure 11. Effect of surface crack with an initial crack depth of 1 mm on fatigue accumulation damage.

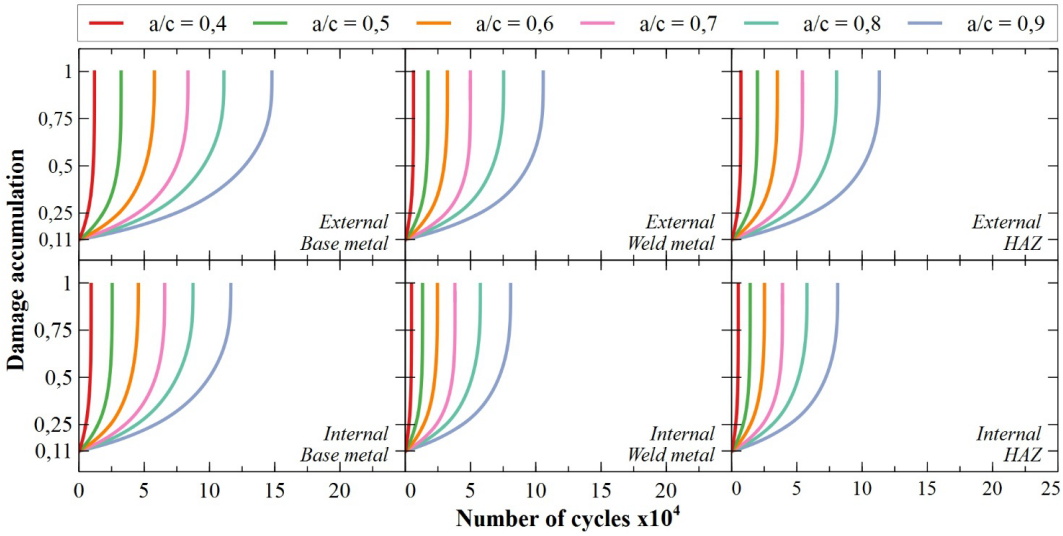

Figure 12. Effect of surface crack with an initial crack depth of 1.5 mm on fatigue accumulation damage.

Using Figure 10 to 13, the fatigue life obtained for each internal crack with a similar crack of the same dimension *a/c = 0.9* is compared to that with an initial depth immediately below. For cracks in the BM, there is a relative difference of -24, -20.13, and -16.77% for cracks with initial depths of 1, 1.5, and 2mm, respectively. For cracks in the WM, the deviation is -26.91, -20.97, and -18.96% for cracks with initial depths of 1, 1.5, and 2 mm, respectively. When it comes to cracks in the HAZ, there is a relative variation of -26.47, -17.88, and -19.16% for cracks at initial depths of 1, 1.5, and 2 mm, respectively. Based on these deviations, it can be seen that increasing the initial crack depth parameter has less of an effect on reducing the fatigue life of the defective structure. The shape of the curves also shows that each curve has a shift to the left when compared to the curve corresponding to a crack of the same dimensions, position, and location but with an initial depth that is immediately lower.

Let us compare the shape of the curves of evolution of damage accumulation for dented pipes (Figure 9) to those for cracked pipes (in Figure 10 to 13). The accumulation of damage is clearly slower in the case of dented pipes subjected to variable amplitude loads. The shape of the evolution of damage accumulation curves increases exponentially with the number of cycles for all types of defects. When compared to the curves obtained for dented pipes, this exponential effect is more pronounced in the case of a cracked pipe. For low damage accumulation values, the slope of the curves obtained for crack defects and that for dent defects is quite close. For high damage accumulation values, however, it is observed that the rate of increase of the slope in the case of a dented pipe remains quasi-constant, whereas the slope in the case of a cracked pipe tends towards infinity. Figure 14 and 15 are used to compare and classify the various defects studied based on their degree of harmfulness in the various stages of damage accumulation evolution.

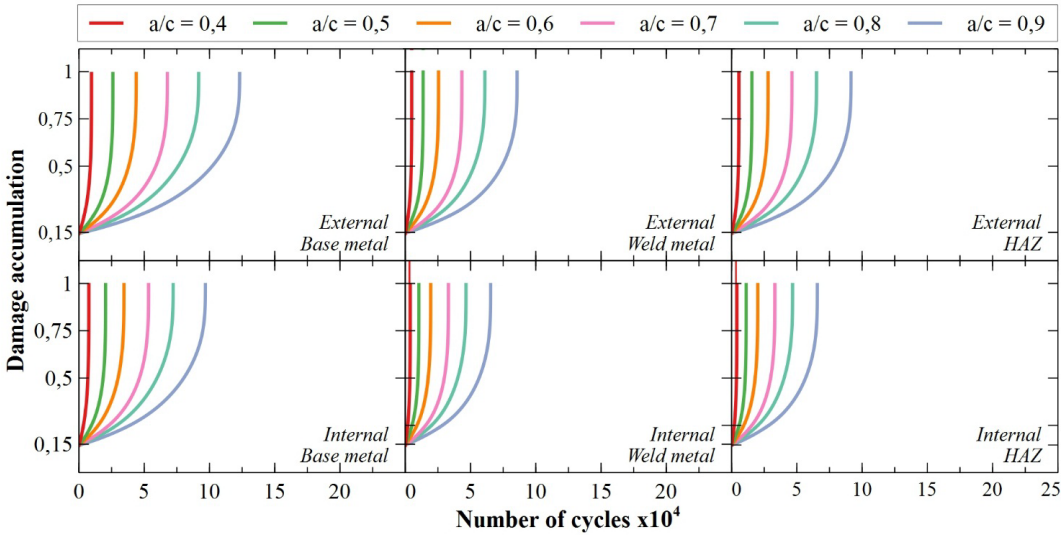

Figure 13. Effect of surface crack with an initial crack depth of 2mm on fatigue accumulation damage.

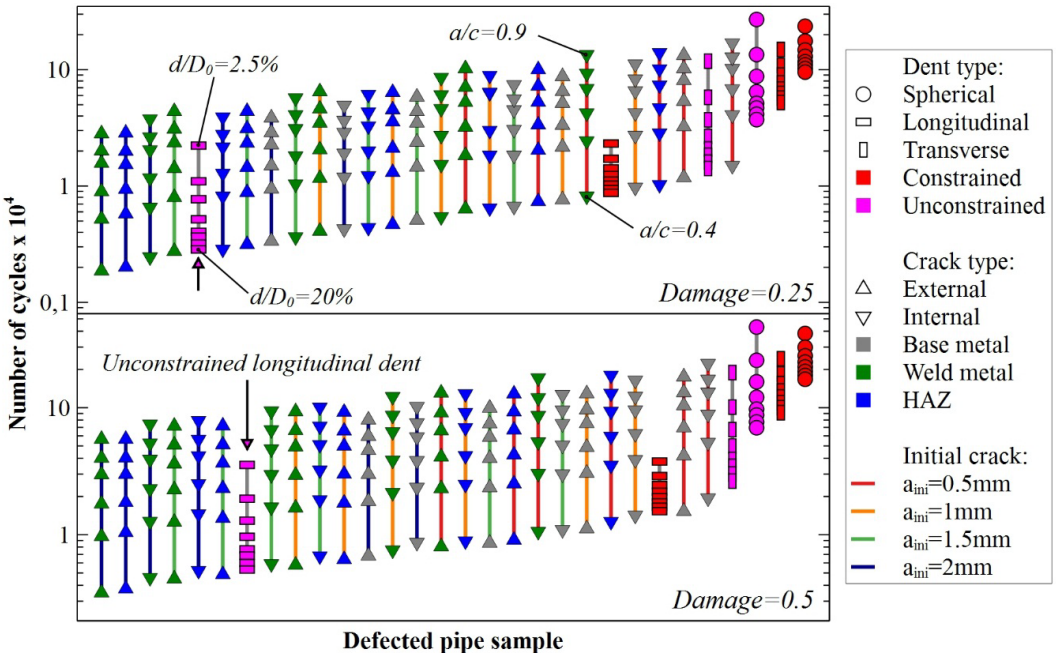

Figure 14. The number of cycles associated with fatigue accumulation damage of 0.25 and 0.5 of the defects investigated.

Based on the findings depicted in Figure 8 to 13, four points were kept for each curve. These points are the intersections of horizontal lines representing damage accumulation values of 0.25, 0.5, 0.75, and 1 with the damage accumulation evolution curve for each type of defect studied. By projecting these points orthogonally on the abscissa axis, the number of cycles corresponding to damage values of 0.25, 0.5, 0.75, and 1 is obtained. All of these values are depicted in Figures 14 and 15, with the cases of a defect causing the fewest number of fatigue cycles appearing first. It should be noted that the y-axis in these figures is on a logarithmic scale to improve readability. For crack defects, the values of the a/c dimensions are read from the bottom up, from 0.4 to 0.9 with a 0.1 step. For dent defects, the values of the d/D_o dimensions are read from top to bottom, from 2.5% to 20% with a 2.5% step.

These figures not only allow for the classification of the studied defects, but they also allow for the identification of equivalence between these defects, even for different types, and this for several stages of the structure's life. This is made possible by using the parameter of damage accumulation as a common adimensional scale. Without this parameter, it is remarkably difficult to directly compare the harmfulness of various types of defects (cracks and dents).

To demonstrate how these figures can be used, consider the defects framed in Figure 14 and 15. We can conclude from a simple reader that an internal crack defect with an initial depth of 1.5 mm located in the WM is equivalent in harmfulness to an external crack defect with an initial depth of 1mm located in the same zone. This observation holds true for all four stages of life. To find the equivalence in terms of harmfulness for all the studied defects, draw a horizontal line passing through the defect for which the equivalences are sought. If the value of the a/c or d/D_o parameter does not appear in the figure, linear interpolation can be used to approximate it.

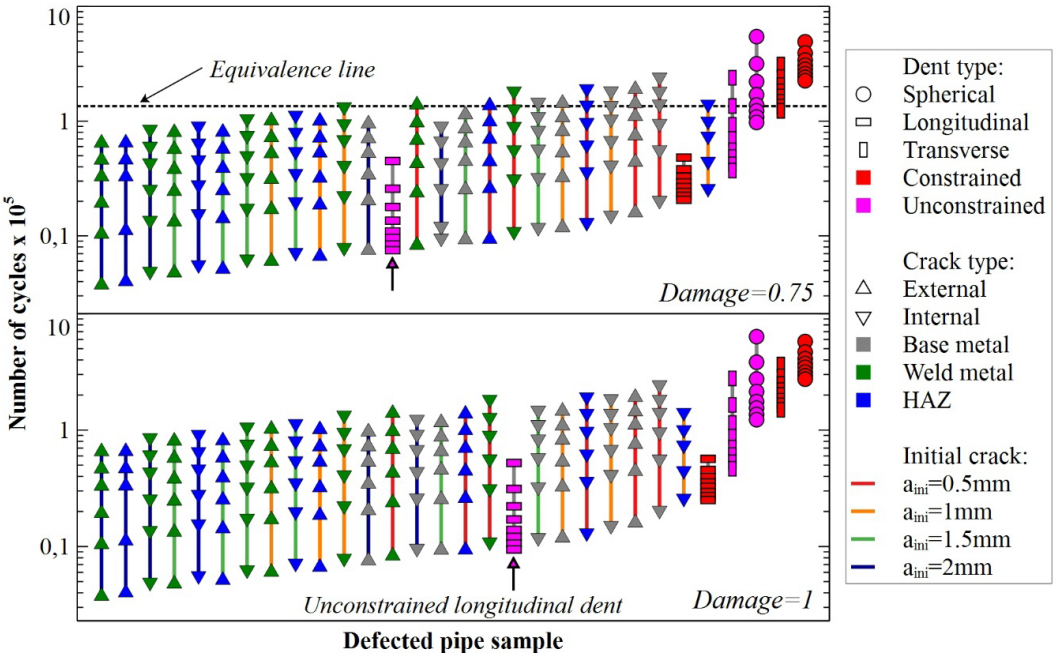

Figure 15. The number of cycles associated with fatigue accumulation damage of 0.75 and 1 of the defects investigated.

Let us use Figure 15 as an example to find the defects equivalent to an unconstrained transverse rectangular indentation of depth d/D_o = 5 %. Draw a horizontal line through the defect (see Figure 15) and examine the intersections of this line with the curves of the various defects. Let us look at some equivalence examples:

i. A constrained transverse rectangular dent defect with a depth of d/D_o = 17.5 %;
ii. An unconstrained spherical dent with a depth d/D_o of 14.375 % (approximated by linear interpolation);
iii. An internal crack defect with a/c dimension of 0.9 in the HAZ with an initial depth of 1 mm;
iv. An internal crack defect with a/c dimension of 0.9 in the BM with an initial depth of 1.5 mm;
v. An external crack defect with a/c dimension of 0.89 (obtained through linear interpolation) in the WM with an initial depth of 0.5 mm.

Figure 14 and 15 show that the unconstrained longitudinal dent defect is one of the most harmful defects in the first phase of the pipe's life. The greater the number of cycles, the less harmful this defect is. In order to better follow the evolution of the harmfulness of this defect, an arrow has been drawn in these figures. It should be noted that the value ranges used by all of the parameters studied are those found in the literature and the field. Figure 14 and 15 show that dent defects are generally less harmful than crack defects, especially near the end of pipe life.

CONCLUSION

In a parametric investigation, a numerical damage accumulation model is utilized to evaluate the nocivity due to the presence of a crack or dent defect in a pipe. This model takes into account the effects of loading history and interaction effect. The pressure spectrum induced by the water hammer, which is caused by an abrupt change in the status of a valve on a water transmission line, is fed into this model. It employs, in its damage calculation process, analytical models derived from studies on interpolation of FEM model findings.

The main purpose of this study is to compare and classify flaws in diverse categories (surface cracks and dents). In the parametric analysis concerning dent defects, the effect of the dent's depth, shape (spherical and rectangular), orientation (longitudinal and transverse), and configuration (constrained and unconstrained) is investigated. The geometry, initial depth, location (external and internal), and position (in the base metal, weld metal, and heat-affected zone) effects on surface crack defects are explored in a parametric study involving cracked pipes.

This research not only allows for the classification of the flaws under investigation but also for the identification of equivalence between them in terms of pipeline damage, even for various categories and at different stages of the structure's life. This is primarily due to the damage accumulation parameter being used as a common adimensional scale. The established numerical model can be used to analyze the harmfulness of various flaws in the pipes with minimal alterations. The same approach can be used to evaluate the impact of other types of structural loading. As a result, equivalences between flaws throughout a wider spectrum can be found.

ACKNOWLEDGEMENT

The authors would like to acknowledge the facilities, scientific and technical support from Signals, Distributed Systems and Artificial Intelligence Laboratory in Higher Normal School of Technical Education of Mohammedia.

REFERENCES

[1] J. Yu, Y. Zhao, T. Li and Y. Yu, "A three-dimensional numerical method to study pipeline deformations due to transverse impacts from dropped anchors," *Thin-Walled Struct.*, vol. 103, pp. 22–32, 2016, doi: 10.1016/j.tws.2016.02.006.

[2] 7th Report of the European Gas Pipeline Incident Data Group, "Gas pipeline incidents," Document No. EGIG 08 TV-B 0502, December 2008.

[3] M. Arefi, M. H. Ghaeini and R. Memarzadeh, "Numerical modeling of water hammer in long water transmission pipeline," *Appl. Water Sci.*, vol. 11, no. 8, pp. 140, 2021, doi: 10.1007/s13201-021-01471-9.

[4] O. Obeid, G. Alfano, H. Bahai and H. Jouhara, "Mechanical response of a lined pipe under dynamic impact," *Eng. Fail. Anal.*, vol. 88, pp. 35–53, 2018, doi: 10.1016/j.engfailanal.2018.02.013.

[5] A. Cosham and P. Hopkins, "The effect of dents in pipelines - guidance in the pipeline defect assessment manual," *Int. J. Press. Vessel. Pip*., vol. 81, no. 2, pp. 127–139, 2004, doi: 10.1016/j.ijpvp.2003.11.004.

[6] A. Okodi *et al.*, "Crack propagation and burst pressure of pipeline with restrained and unrestrained concentric dent-crack defects using extended finite element method, " *Appl. Sci.* vol. 10, no. 21, pp. 7554, 2020, doi: 10.3390/app10217554.

[7] M. Kandil, A. M. Kamal and T. El-Sayed, "Effect pipes material on water hammer," *Int. J. Press. Vessel. Pip.*, vol. 179, 2019, doi: 10.1016/j.ijpvp.2019.103996.

[8] A. Kodura, P. Stefanek and K. Weinerowska-Bords, "An experimental and numerical analysis of water hammer phenomenon in slurries," *J. Fluids Eng.*, vol. 139, no. 12, pp. 1–9, 2017, doi:10.1115/1.4037678.

[9] F. Yue and W. Ziyan, "Fracture mechanical analysis of thin-walled cylindrical shells with cracks," *Metals*, vol. 11, no. 4, pp. 592, 2021, doi: 10.3390/met11040592.

[10] I. Zhuravska, D. Lernatovych and O. Burenko, "Detection the places of the heat energy leak on the underground thermal pipelines using the computer system," *Adv. Sci. Technol. Eng. Syst.*, vol. 4, no. 3, pp. 01–09, 2019, doi: 10.25046/aj040301.

[11] A. Vojdani and G. Farrahi, "Reliability assessment of cracked pipes subjected to creep-fatigue loading," *Theor. Appl. Fract. Mech.*, vol. 104, pp. 1–12, 2019, doi: 10.1016/j.tafmec.2019.102333.

[12] H. Gao *et al.*, "A modified nonlinear damage accumulation model for fatigue life prediction considering load interaction effects," *Sci. World J.*, vol. 2014, pp. 1–8, 2014, doi: 10.1155/2014/164378.

[13] S. B. Cunha, I. Pasqualino and B. Pinheiro, "Pipeline plain dent fatigue – A comparison of assessment methodologies," In. Proc. 10th International Pipeline Conference, Calgary, Alberta, Canada, 2014, doi: 10.13140/2.1.4112.8326.

[14] Z. Mustaffa *et al.*, "Reliability assessment for corroded pipelines in series considering length-scale effects," *Int. J. Automot. Mech. Eng.*, vol. 15, no. 3, pp. 5607–5624, 2018, doi: 10.15282/ijame.15.3.2018.16.0431.

[15] A. Fezazi, B. Mechab, M. Salem and B. Serier, "Numerical prediction of the ductile damage for axial cracks in pipe under internal pressure," *Frattura ed Integrità Strutturale*, vol. 15, pp. 231-241, 2021, doi: 10.3221/IGF-ESIS.58.17.

[16] Z. Mighouar *et al.*, "Effect of water hammer on pipes containing a crack defect," *Int. J. Mech. Mechatron. Eng.*, vol. 18, no. 3, pp. 25–31, 2018.

[17] L. Zahiri *et al.*, "Fatigue life analysis of dented pipes subjected to internal pressure," *Int. Rev. Mech. Eng.*, vol. 11, no. 8, pp. 587–596, 2017, doi: 10.15866/ireme.v11i8.12089.

[18] L. Zahiri *et al.*, "Fatigue behavior of longitudinal welded pipes subjected to cyclic internal pressure, containing welding defects," *Int. J. Mech. Eng.,* vol. 9, no. 3, pp. 560–569, 2018.

[19] Z. Mighouar, L. Zahiri, H. Khatib and K. Mansouri, "Damage accumulation model for cracked pipes subjected to water hammer," *Adv. Sci. Technol. Eng. Syst.,* vol. 5, pp. 523–530, 2020, doi: 10.25046/aj050462.

[20] Z. Mighouar, H. Khatib, L. Zahiri and K. Mansouri, "Damage accumulation model of a dented pipeline subject to water hammer waves," *Int. Rev. Mech. Eng.*, vol. 14, no. 12, pp. 730–742, 2020, doi: 10.15866/ireme.v14i12.20348.

[21] G. Anderson *et al.*, "ASME B16.9 piping components: An analysis of the critical dimensions," In Proc. SIMS Conference on Simulation and Modelling, pp. 222–228, 2021, doi: 10.3384/ecp20176222.

[22] M. J. Rosenfeld, "Development of a model for fatigue rating shallow unrestrained dents," Pipeline Research Council International, no. L51741, PRCI Report PR-218-9405, 1997.

[23] C. R. Alexander, "Analysis of dented pipeline considering constrained and unconstrained dent configurations," presented at Energy Sources Technology Conference & Exhibition, Houston, Texas. 1999.

[24] "DIN 2413 Part 1, Design of steel pressure pipes," Deutshe Norm, 1993.

[25] "Boiler and pressure vessel code, Section VIII, Division 2," American Society of Mechanical Engineers (ASME), 1995.

[26] A. Cosham, R. Andrews and T. Schmidt, "The EPRG recommendations for crack arrest toughness for line pipe steel," In Proc. of 12th International Pipeline Conference, 2018, pp. 1–11, 2018, doi:10.1115/IPC2018-78043.

[27] B. D. Carvalho, I. P. Pasqualino and S. B. Cunha, "Stress concentration factors of dented pipelines," In Proc. Intern. Pipeline Conf., no. 10598, pp. 335-344, 2006.

[28] B. Pinheiro, C. Guedes Soares and I. Pasqualino, "Generalized expressions for stress concentration factors of pipeline plain dents under cyclic internal pressure," *Int. J. Press. Vessel. Pip.*, vol. 170, pp. 82-91, 2019, doi: 10.1016/j.ijpvp.2019.01.015.

[29] S. Cunha, I. Pasqualino and B. Pinheiro, "Stress-life fatigue assessment of pipelines with plain dents," *Fatigue Fract. Eng. Mater. Struct.* vol. 32, pp. 961–974, 2009, doi: 10.1111/j.1460-2695.2009.01396.x.

[30] J. O. Jajo, "Dent behaviour of steel pipes under pressure load," Ph.D. dissertation, University of Windsor, Windsor, 2011.

[31] C. Narváez-Tovar *et al.*, "Fatigue crack growth and fracture toughness in a dual phase steel: effect of increasing martensite volume fraction," *Int. J. Automot. Mech. Eng.*, vol. 17, pp. 8086–8095, 2020, doi: 10.15282/ijame.17.3.2020.02.0606.

[32] S. H. Jeong *et al.*, "On elastic-plastic and creep fracture mechanics parameters estimates of non-idealized axial through-wall crack in pressurized pipe," *Int. J. Press. Vessel. Pip.*, vol. 189, no. 104292, 2021, doi: 10.1016/j.ijpvp.2020.104292.

[33] R. Pippan and A. Hohenwarter, "Fatigue crack closure: a review of the physical phenomena," *Fatigue Fract. Eng. Mater. Struct.*, vol. 40, no. 4, pp. 471-495, 2017, doi: 10.1111/ffe.12578.

[34] P. C. Paris and F. Erdogan, "A critical analysis of crack propagation laws," *J. Basic Eng.*, vol. 85, pp. 528–533, 1963, doi: 10.1115/1.3656900.

[35] W. Elber, "Fatigue crack closure under cyclic tension," *Eng. Fract. Mech.,* vol. 2, no. 1, pp. 37–45, 1970, doi: 10.1016/0013-7944(70)90028-7.

[36] W. Wang, "On the finite width correction factor in prediction models for fatigue crack growth in built-up bonded structures," *Eng. Fract. Mech.,* vol. 235, 2020, doi: 10.1016/j.engfracmech.2020.107156.
[37] N. Paruolo, B. Pinheiro, T. Mello and I. Pasqualino, "Stress concentration factors on welded tubular joints," *Practical Design of Ships and Other Floating Structures*, vol. 64, pp. 681–700, 2021, doi: 10.1007/978-981-15-4672-3_42.
[38] E. Buckingham, "On physically similar systems, illustration and the use of dimensional equations," *Physical Review*, vol. 4(4), pp. 345–376, 1914, doi: 10.1103/PhysRev.4.345.
[39] Z. Y. Jin, X. Wang, D. J. Yu and X. Chen, "The effects of nonproportional loading on the elastic-plastic crack-tip fields," *Appl. Mech. Mater.,* vol. 853, pp. 83–87, 2016, doi: 10.4028/www.scientific.net/amm.853.83.
[40] J. C. Newman, "Fracture analysis of surface- and through-cracked sheets and plates," *Eng. Fract. Mech.*, vol. 5, no. 3, pp. 667–689, 1973, doi: 10.1016/0013-7944(73)90046-5.
[41] B. Mechab, N. Chioukh, B. Mechab and B. Serier, "Probabilistic fracture mechanics for analysis of longitudinal cracks in pipes under internal pressure," *J. Fail. Anal. Prev.*, vol. 18, no. 6, pp. 1643–1651, 2018, doi: 10.1007/s11668-018-0564-8.
[42] M. El-Sayed, A. E. Domiaty and A-H. I. Mourad, "Fracture assessment of axial crack in steel pipe under internal pressure," *Procedia Eng.*, vol. 130, pp. 1273–1287, 2015, doi: 10.1016/j.proeng.2015.12.297.
[43] Y. Peng, C. Wu, Y. Zheng and J. Dong, "Improved formula for the stress intensity factor of semi-elliptical surface cracks in welded joints under bending stress," *Materials (Basel)*, vol. 10, no. 2, pp. 166, 2017, doi: 10.3390/ma10020166.
[44] A. Benin, S. Nazarova and A. Uzdin, "Designing scenarios of damage accumulation," In Proc. International Scientific Conference Energy Management of Municipal Facilities and Sustainable Energy Technologies, pp 600–610, 2019, doi: 10.1007/978-3-030-19868-8_57.
[45] A. Belegundu, S. Nayak, J. Loverich and M. Grissom, "Vibration-based damage accumulation modeling," In Proc. 28th Conf. on Mechanical Vibration and Noise, North Carolina, USA, 2016, doi: 10.1115/DETC2016-59106.
[46] H. Thun, U. Ohlsson and L. Elfgren, "A deformation criterion for fatigue of concrete in tension, " *Struct. Concr.*, vol. 12, no. 3, pp. 187–197, 2011, doi: 10.1002/suco.201100013.